

# Influence of substitution of phenyl group by naphthyl in a diphenylthiourea molecule on corrosion inhibition of cold-rolled steel in 0.5 M H<sub>2</sub>SO<sub>4</sub>

O. Benali · L. Larabi · S. M. Mekelleche · Y. Harek

Received: 4 September 2005 / Accepted: 6 December 2005 / Published online: 12 October 2006  
© Springer Science+Business Media, LLC 2006

**Abstract** *N,N'*-Diphenylthiourea (DPTU) and *N*-naphthyl-*N'*-phenylthiourea (NPTU) synthesized in our laboratory, were tested as inhibitors for the corrosion of cold-rolled steel in 0.5 M H<sub>2</sub>SO<sub>4</sub> by weight loss and electrochemical measurements. The studies clearly reveal that when we substitute a phenyl group in *N,N'*-diphenylthiourea (DPTU) by naphthyl group to obtain *N*-naphthyl-*N'*-phenylthiourea (NPTU), the inhibition efficiency increases from 80 to 96% at  $2 \times 10^{-4}$  M. Polarization curves show that NPTU acts as mixed type inhibitor whereas DPTU predominates as cathodic inhibitor. Changes in impedance parameters (charge transfer resistance,  $R_t$ , and double layer capacitance,  $C_{dl}$ ) were indicative of adsorption of DPTU and NPTU on the metal surface, leading to the formation of protective films. The degree of the surface coverage of the adsorbed inhibitors is determined by ac impedance technique, and it was found that the adsorption of these inhibitors on the cold-rolled steel surface obeys the Langmuir adsorption isotherm. The effect of the temperature on the corrosion behavior with addition of  $10^{-4}$  M of DPTU and NPTU was studied in the temperature range 20–50 °C. Results show that the rate of corrosion of mild steel increased with increasing temperature both in the presence of inhibitors and in their absence. Activation energies in the presence and absence of DPTU and NPTU were obtained by measuring the temperature dependence of

the corrosion current. The reactivity of these compounds was analyzed through theoretical calculations based on density functional theory to explain the different efficiency of these compounds as corrosion inhibitors.

## Introduction

As we know, carbon steel is widely used as a constitutional material in many industries due to its good mechanical properties and low cost. The corrosion of carbon steel is of fundamental academic and industrial concern that has received a considerable amount of attention. Acid pickling baths are employed to remove undesirable scale from the surface of the metals. Once the scale is removed, the acid is then free for further attack on the metal surface. The use of inhibitor is one of the most practical methods for protection against corrosion, especially in acidic media.

A survey of literature reveals that the applicability of organic compounds as corrosion inhibitors for steel in acidic media has been recognized for a long time. Compounds studied as inhibitors include triazole derivatives [1–5], bipyrazolic derivatives [6], surfactants [7, 8] aromatic hydrazides [9], organic dyes [10, 11], Poly(4-vinylpyridine) [12–15] and thiosemicarbazide-type organic compounds [16–20]. These compounds can adsorb on the steel surface and block the active sites decreasing the corrosion rate.

The aim of this work is to study the inhibition efficiency of sulfur-based inhibitors like *N*-naphthyl-*N'*-phenylthiourea (NPTU) and *N,N'*-diphenylthiourea

O. Benali  
Département de biologie, Centre universitaire de Saïda,  
20000 Saïda, Algérie

L. Larabi (✉) · S. M. Mekelleche · Y. Harek  
Département de Chimie, Faculté des sciences, Université  
Abou Bakr Belkaid, 13000 Tlemcen, Algérie  
e-mail: larabi\_lahcene@yahoo.fr

(DPTU) on cold-rolled steel in acidic media. The behavior of these compounds in 0.5 M  $H_2SO_4$  has been studied using chemical (weight loss) and electrochemical (potentiodynamic polarization, linear polarization, electrochemical impedance spectroscopy) techniques. The adsorption behavior of the inhibitors was studied and thermodynamic function for dissolution and adsorption process were calculated and discussed. The effect of the substitution of phenyl group by naphthyl group on the performance of DPTU, as a corrosion inhibitor of cold-rolled steel, has been studied. Theoretical calculations based on the potential ionization and the Fukui indices [21], which are descriptors derived from density functional theory (DFT), were performed, in order to give further insight into the experimental results.

## Experimental

### Materials

Cold-rolled steel composed of (in wt.%)  $C \leq 0.15$ ,  $Mn \leq 0.50$ ,  $P \leq 0.03$ ,  $S \leq 0.03$  and the remainder iron was used as the working electrode for all studies.

Inhibitors were synthesized in the laboratory by condensation of phenyl isothiocyanate with appropriate amine and were purified and analyzed by IR and NMR spectroscopies before use. Figure 1 shows the molecular structures of the investigated organic compounds which have been labeled DPTU and NPTU. The acid solutions were made from AR grade  $H_2SO_4$ . Appropriate concentration of acid was prepared by using double-distilled water.

### Weight loss measurements

For the weight loss measurements, the experiments were carried out in solution of 0.5 M sulfuric acid (uninhibited and inhibited) on cold-rolled steel. Sheets with dimensions  $15 \times 15 \times 1.5$  mm were used. They were polished successively with different grades of emery paper up 1000 grade. Each run was carried out in a glass vessel containing 50 ml test solution. A clean weight cold-rolled steel sample was completely immersed at an inclined position in the vessel. After 2 h of immersion in 0.5 M  $H_2SO_4$  with and without addition of inhibitor at different concentrations, the specimen was withdrawn, rinsed with distilled water, washed with ethanol, dried and weighted. The weight loss was used to calculate the corrosion rate in milligrams per square centimeter per hour.

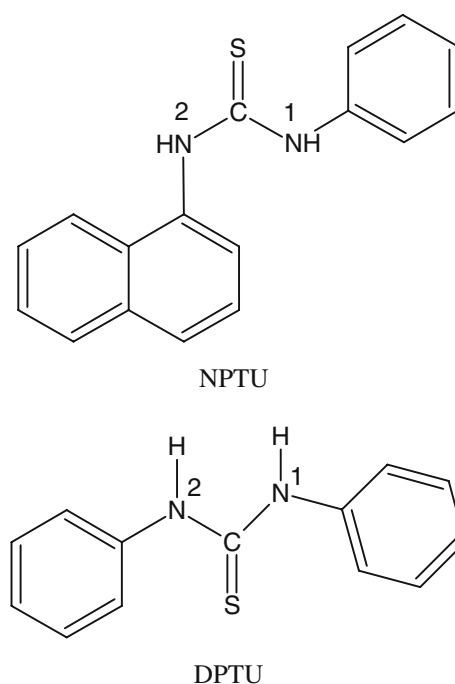


**Fig. 1** Molecular structures of NPTU and DPTU

### Electrochemical measurements

Electrochemical experiments were carried out in a glass cell (CEC/TH-Radiometer) with a capacity of 500 ml. A platinum electrode and a saturated calomel electrode (SCE) were used as a counter electrode and a reference electrode. The working electrode (WE) was in the form of a disc cut from mild steel under investigation and was embedded in a Teflon rod with an exposed area of  $0.5 \text{ cm}^2$ .

Electrochemical impedance spectroscopy (EIS), potentiodynamic and linear polarization were conducted in an electrochemical measurement system (VoltaLab40) which comprises a PGZ301 potentiostat, a personal computer and VoltaMaster 4 and Zview software.

The potentiodynamic current–potential curves were recorded by changing the electrode potential automatically from  $-700$  to  $-250$  mV with scanning rate of  $0.5 \text{ mV s}^{-1}$ . The polarization resistance measurements were performed by applying a controlled potential scan over a small range typically 15 mV with respect to  $E_{\text{corr}}$ . The resulting current is linearly plotted versus potential, the slope of this plot at  $E_{\text{corr}}$  being the polarization resistance ( $R_p$ ). All experiments were carried out in freshly prepared solution at constant temperatures, 20, 30,  $40^\circ\text{C}$  and  $50 \pm 0.1^\circ\text{C}$  using a thermostat.

The ac impedance measurements were performed at corrosion potentials ( $E_{\text{corr}}$ ) over a frequency range of 10 kHz–20 mHz, with a signal amplitude perturbation of 10 mV. Nyquist plots were obtained.

## Theoretical calculations

The equilibrium geometries of the NPTU and DPTU molecules were optimized by the AM1 semi-empirical method [22] implemented in Mopac program [23]. The atomic electronic populations were calculated at the B3LYP/6-31G\* level of theory using Gaussian 94W package [24]. The chemical reactivity of the different sites of the molecules was evaluated by Fukui indices, which are defined by [21]

$$f_k^+ = [q_k(N+1) - q_k(N)] \quad (1)$$

for nucleophilic attack, and

$$f_k^- = [q_k(N) - q_k(N-1)] \quad (2)$$

for electrophilic attack

where  $q_k(N)$ ,  $q_k(N-1)$ , and  $q_k(N+1)$  denote electronic populations of the atom  $k$  in neutral, cationic, and anionic systems, respectively. These quantities were calculated using Mulliken Population Analysis [25].

The ionization potentials were calculated as the difference between cationic and neutral systems using the B3LYP/6-31G\* correlation method.

## Results and discussion

### Polarization measurements

Potentiodynamic anodic and cathodic polarization scans were carried out at  $30 \pm 0.1$  °C in 0.5 M  $H_2SO_4$  with different concentrations of DPTU and NPTU. Anodic and cathodic polarization curves in the absence and in the presence of inhibitors at different concentrations after 1 h of immersion and at 30 °C are shown in Figs. 2 and 3. In the presence of both inhibitors at all the concentrations studied a decrease in cathodic current is noted. In the case of NPTU, the anodic current decreases with increasing the concentration of the inhibitor, while in the case of DPTU, the anodic current decreases in a small potential range at higher inhibitor concentrations only. This is attributed to the better covering effect of NPTU molecule at the electrode surface than that of DPTU.

Furthermore, we remark that when the DPTU concentrations are  $2.5 \times 10^{-5}$  and  $5 \times 10^{-5}$  M, the anodic currents nearby the corrosion potential are higher than that measured in the blank solution. This can be explained as follows: it is known that the organic sulfur-containing compounds have two opposite effects

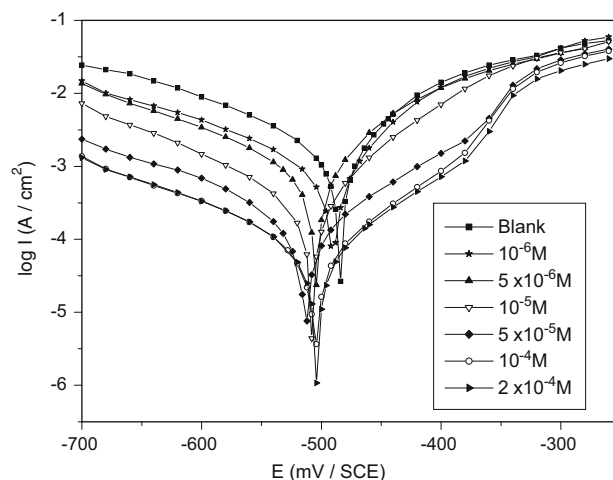


**Fig. 2** Potentiodynamic polarization curves for cold-rolled steel in 0.5 M  $H_2SO_4$  containing different concentrations of NPTU at 30 °C

on the corrosion of iron and steels. On the one hand, they can chemisorb on the surface of iron and steels, segregate the metal surface from the solution and therefore inhibit the corrosion of iron and steels. On the other hand, some of the organic sulfur-containing compound molecules adsorbed on the surface of iron may decompose and give out  $H_2S$ , which can accelerate the corrosion of iron and steel in acid solutions [26]. Thus, when the concentration of DPTU in the solution is fairly low, the anodic dissolution of steel was accelerated by the  $H_2S$  decomposed from DPTU.

Moreover, for anodic polarization, currents increased with potential, especially at high overpotentials and

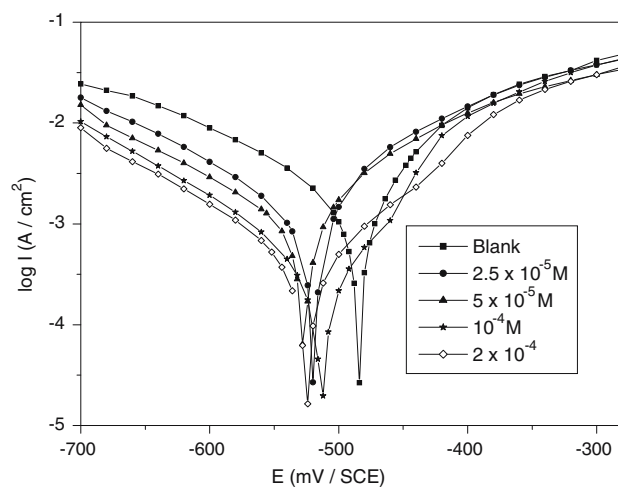


**Fig. 3** Potentiodynamic polarization curves for cold-rolled steel in 0.5 M  $H_2SO_4$  containing different concentrations of DPTU at 30 °C

concentrations; this is probably caused by the increase in surface area, as cold-rolled steel dissolves and organic molecules desorb, above which the coverage of inhibitors decreases rapidly [27]. The values of various electrochemical parameters are summarized in Table 1.

The values of the corrosion potentials were only slightly shifted by addition of NPTU, for example, for the concentration of  $2 \times 10^{-4}$  M of NPTU, concentration for which the current densities are weaker, we get  $E_{\text{corr}}$  equals to  $-505$  mV/SCE, which is near of the value obtained in the reference case ( $-490$  mV/SCE). This result suggests that NPTU acts as relatively mixed inhibitor. In the case of DPTU, the cathodic shift of  $E_{\text{corr}}$  indicates that the cathodic process is much more affected than the anodic process. Moreover, DPTU has little effect when the potential became more positive than  $E_{\text{corr}}$ . Thus the inhibition of corrosion of cold-rolled steel in under cathodic control and DPTU is predominately a cathodic inhibitor. On the other hand, the cathodic slope values are almost same with and without the presence of inhibitors studied in  $0.5$  M  $\text{H}_2\text{SO}_4$ , which indicates that hydrogen evolution reaction is activation controlled and that the inhibitors adsorb by simple blocking the active sites of the metal surface.

The corrosion current densities were estimated by Tafel extrapolation of the cathodic curves to the open circuit corrosion potentials. The inhibition efficiency was then calculated using the expression

$$P\% = \frac{I_u - I_i}{I_u} \times 100 \tag{3}$$

where  $I_u$  is the corrosion current density in uninhibited acid and  $I_i$  is the corrosion current density in inhibited acid.

Table 1 shows that an increase in inhibitor concentration is resulted in increased inhibition efficiency. It is evident from the results that the  $I_{\text{corr}}$  values decrease considerably in the presence of inhibitor. Thus,  $P$  (%) increases with inhibitor concentration, reaching the

values 96 and 80% at  $2 \times 10^{-4}$  M of NPTU and DPTU, respectively. About  $2 \times 10^{-4}$  M is the maximum of solubility of the tested compounds. It can also be seen from Table 1 that the corrosion inhibition ability of the compounds listed is greater for NPTU than for DPTU.

Linear polarization technique was performed in  $0.5$  M  $\text{H}_2\text{SO}_4$  with various concentrations of NPTU and DPTU. The corresponding polarization resistance ( $R_p$ ) values of cold-rolled steel in the absence and in the presence of different inhibitor concentrations are also given in Table 1. It is apparent that  $R_p$  increases with increasing inhibitor concentration. The inhibition percentage ( $P\%$ ) calculated from  $R_p$  values are also presented in Table 1. We remark that  $P\%$  increases with increasing concentration of inhibitor and attains 96.4 and 80.4% at  $2 \times 10^{-4}$  M of NPTU and DPTU, respectively. Therefore, the results obtained show that the inhibiting action of NPTU is more pronounced than that of DPTU. The inhibition efficiency of corrosion of cold-rolled steel is calculated by polarization resistance as follows:

$$P\% = \frac{R' - R}{R'} \times 100 \tag{4}$$

where  $R$  and  $R'$  are the polarization resistance values without and with inhibitor, respectively.

The inhibition efficiencies of inhibitors obtained by potentiodynamic polarization and by polarization resistance methods are in good agreement.

### AC impedance studies

Nyquist plots of cold-rolled steel in  $0.5$  M  $\text{H}_2\text{SO}_4$  in the presence and absence of additives are given in Figs. 4 and 5. These curves have obtained after 1 h of immersion in the corresponding solution. All the plots display a single capacitive loop. Impedance parameters derived from the Nyquist plots, percent inhibition efficiencies,  $P$  (%) and the equivalent circuit diagram

**Table 1** Electrochemical parameters and the corresponding corrosion inhibition efficiencies for the corrosion of cold-rolled steel in  $0.5$  M  $\text{H}_2\text{SO}_4$  containing different concentrations of NPTU and DPTU at 303 K

	Conc. (M)	$E_{\text{corr}}$ (mV/SCE)	$I_{\text{corr}}$ ( $\mu\text{A cm}^{-2}$ )	$b_c$ (mV $\text{dec}^{-1}$ )	$R_p$ ( $\Omega \text{ cm}^2$ )	$P_I$ (%)	$P_R$ (%)
Blank		-490	2140	179	10.6	–	–
NPTU	$1 \times 10^{-6}$	-490	955	180	27.3	55.4	61.2
	$5 \times 10^{-6}$	-500	758	164	30.8	65.6	65.5
	$1 \times 10^{-5}$	-505	390	160	62.1	81.8	83
	$5 \times 10^{-5}$	-510	224	183	140	89.5	92.4
	$1 \times 10^{-4}$	-503	95.5	178	267.3	95.5	96
	$2 \times 10^{-4}$	-505	85	179	297.2	96	96.4
DPTU	$2.5 \times 10^{-5}$	-520	1550	172	16.3	27.6	35.0
	$5 \times 10^{-5}$	-520	1130	167	21.6	47.2	50.9
	$1 \times 10^{-4}$	-511	480	143	52.4	77.6	79.8
	$2 \times 10^{-4}$	-525	420	152	54.0	80.4	80.4

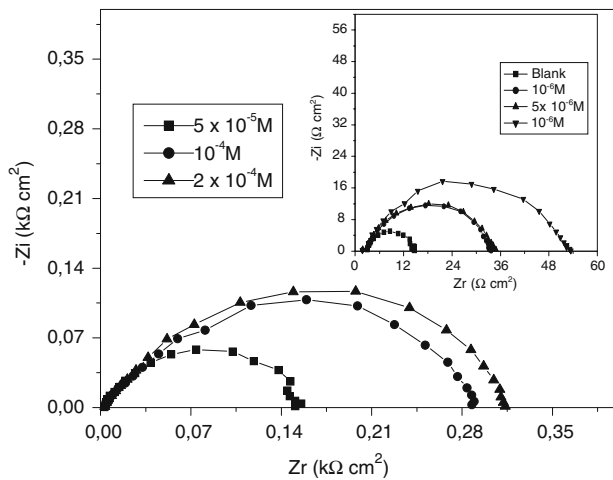


**Fig. 4** Nyquist plots for cold-rolled steel in 0.5 M  $\text{H}_2\text{SO}_4$  containing different concentrations of NPTU at 30 °C

are given in Table 2 and Fig. 6, respectively. The circuit consists of a constant phase element (CPE)  $Q$ , in parallel with a resistor  $R_t$ . The use of CPE-type impedance has been extensively described in [28–30]

$$Z_{\text{CPE}} = [Q(j\omega)^n]^{-1} \quad (5)$$

The above equation provides information about the degree of non-ideality in capacitance behavior. Its value makes it possible to differentiate between the behavior of an ideal capacitor ( $n = 1$ ) and of a CPE ( $n < 1$ ).

The percent inhibition efficiency is calculated by charge transfer resistance obtained from Nyquist plots, according to the equation

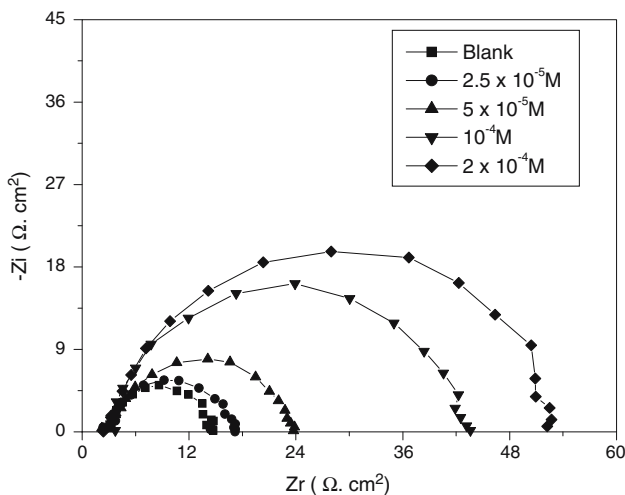


**Fig. 5** Nyquist plots for cold-rolled steel in 0.5 M  $\text{H}_2\text{SO}_4$  containing different concentrations of DPTU at 30 °C

$$P\% = \frac{R'_t - R_t}{R'_t} \times 100 \quad (6)$$

where  $R_t$  and  $R'_t$  are the charge transfer resistance values without and with inhibitor, respectively.

Considering that a CPE may be considered as a parallel combination of a pure capacitor and a resistor that is inversely proportional to the angular frequency, the value of capacitance,  $C_i$ , can thus be calculated for a parallel circuit composed of a CPE ( $Q$ ) and a resistor ( $R_t$ ), according to the following formula [31, 32]:

$$Q = \frac{(CR_t)^n}{R_t} \quad (7)$$

The impedance spectra of cold-rolled steel in 0.5 M  $\text{H}_2\text{SO}_4$  with and without inhibitors were analyzed by using the circuit in Fig. 6, and the double layer capacitance ( $C_{dl}$ ) was calculated in terms of Eq. 7. Values of elements of the circuit corresponding to different corrosion systems, including values of  $C_{dl}$ , are listed in Table 2. As can be seen from this table the increase in resistance in the presence of NPTU and DPTU (compared to  $\text{H}_2\text{SO}_4$  alone) is related to the corrosion protection effect of the molecules. The value of  $C_{dl}$  decreases in the presence of these inhibitors, suggesting that the NPTU and DPTU molecules function by adsorption at the metal solution/interface. It is important to point out that, in all the case of DPTU,  $n$  reaches approximately the same value of 0.88. This result can be interpreted as an indication of the degree of heterogeneity of the metal surface, corresponding to a small depression of the double layer capacitance semicircle. In the presence of NPTU,  $n$  decreases with the increase of the concentration and reaches a value of 0.78. This shows an increase of the surface inhomogeneity as a result of the inhibitor's adsorption.

On the other hand, it can be observed from Table 2 that the electrode impedance of NPTU is higher than that of DPTU. Thus, the effect of molecular structure on inhibition efficiency is the same as that determined by using polarization measurements.

#### Weight loss measurements

Values of the inhibition efficiency and corrosion rate obtained from the weight loss measurements of cold-rolled steel for different concentrations of NPTU and DPTU in 0.5 M  $\text{H}_2\text{SO}_4$  at 30 °C after 2 h of immersion are given in Table 3. The inhibition efficiency is defined as follows:

**Table 2** Impedance parameters and inhibition efficiency for the corrosion of cold-rolled steel in 0.5 M H<sub>2</sub>SO<sub>4</sub> containing different concentrations of NPTU and DPTU at 303 K

	Conc. (M)	R <sub>t</sub> (Ω cm <sup>2</sup> )	Q (Ω <sup>-1</sup> cm <sup>-2</sup> s <sup>n</sup> )	n	C <sub>dl</sub> (μF cm <sup>-2</sup> )	P (%)
Blank		12.5	13.5 × 10 <sup>-5</sup>	0.88	57	–
NPTU	1 × 10 <sup>-6</sup>	32	16.6 × 10 <sup>-5</sup>	0.83	57	60.9
	5 × 10 <sup>-6</sup>	35	15.9 × 10 <sup>-5</sup>	0.82	46	64.3
	1 × 10 <sup>-5</sup>	52.6	17.3 × 10 <sup>-5</sup>	0.78	17	76.2
	5 × 10 <sup>-5</sup>	155	6.28 × 10 <sup>-5</sup>	0.78	14	91.3
	1 × 10 <sup>-4</sup>	288	4.28 × 10 <sup>-5</sup>	0.79	13	95.7
DPTU	2 × 10 <sup>-4</sup>	313	3.76 × 10 <sup>-5</sup>	0.81	13	96
	2.5 × 10 <sup>-5</sup>	16.5	15.3 × 10 <sup>-5</sup>	0.86	58	32
	5 × 10 <sup>-5</sup>	23.8	12.2 × 10 <sup>-5</sup>	0.86	48	47.5
	1 × 10 <sup>-4</sup>	44.5	7.2 × 10 <sup>-5</sup>	0.86	38	71.9
	2 × 10 <sup>-4</sup>	52.8	7.1 × 10 <sup>-5</sup>	0.87	31	76.3

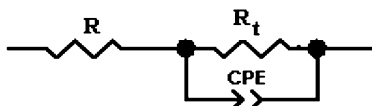


**Fig. 6** The equivalent circuit of the impedance spectra obtained for NPTU and DPTU

$$P\% = \frac{W - W'}{W} \times 100 \tag{8}$$

where *W* and *W'* are the corrosion rates of steel due to the dissolution in 0.5 M H<sub>2</sub>SO<sub>4</sub> in the absence and the presence of definite concentration of inhibitor, respectively.

NPTU and DPTU inhibit the corrosion of cold-rolled steel. It can be seen from Table 3 that inhibition efficiency increases with the increasing inhibitors concentration. Maximum *P*% of each compound was achieved at 2 × 10<sup>-4</sup> M but better performances are seen of the case of NPTU. These results clearly reveal the beneficial effect of the substitution of a phenyl group in DPTU by naphthyl group in NPTU. At 10<sup>-4</sup> M the value of the inhibition efficiency jumps from 78.8% in the presence of DPTU to 93.2% in the presence of NPTU. These results are in reasonably good agreement with the values of inhibitor efficiency obtained from electrochemical techniques.

**Table 3** Corrosion rate of cold-rolled steel and inhibition efficiency for different concentrations of NPTU and DPTU for the corrosion of carbon steel in 0.5 M H<sub>2</sub>SO<sub>4</sub>

	Conc. (M)	V <sub>corr</sub> (mg cm <sup>-2</sup> h <sup>-1</sup> )	P (%)
Blank		0.850	–
NPTU	5 × 10 <sup>-5</sup>	0.094	88.9
	1 × 10 <sup>-4</sup>	0.058	93.2
	2 × 10 <sup>-4</sup>	0.047	94.5
DPTU	5 × 10 <sup>-5</sup>	0.180	78.1
	1 × 10 <sup>-4</sup>	0.186	78.8
	2 × 10 <sup>-4</sup>	0.107	87.4

Adsorption consideration

It is known that the adsorption isotherms are very important for the understanding of the mechanism of corrosion inhibition [33]. The most frequently used isotherms are Langmuir, Freundlich, Temkin, Frumkin, etc. Assuming a direct relationship between inhibition efficiency and surface coverage, *θ*, of the inhibitor, electrochemical impedance spectroscopy data were used to evaluate the surface coverage values, which are given by Eq. 9 [34]

$$\theta = \frac{R'_t - R_t}{R'_t} \tag{9}$$

where *R<sub>t</sub>* and *R'<sub>t</sub>* are the charge transfer resistance values without and with inhibitor, respectively.

The surface coverage values (*θ*) were tested graphically to allow fitting of a suitable adsorption isotherm. The plot of *C/θ* versus *C* (Fig. 7) yielded straight lines with slopes equal to 1.02 and 1.00 for NPTU and DPTU, respectively, clearly proving that the adsorption of the NPTU and DPTU from 0.5 M H<sub>2</sub>SO<sub>4</sub>

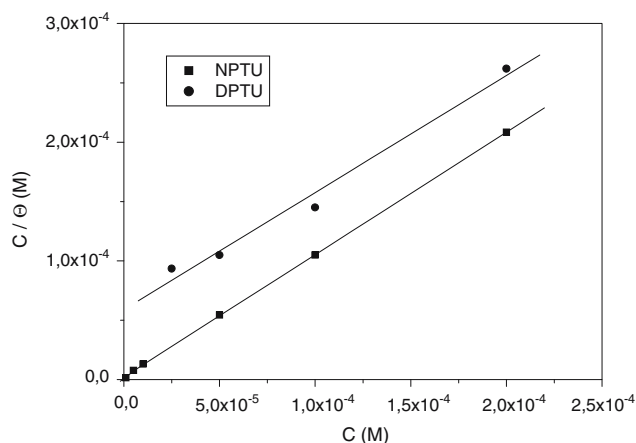


**Fig. 7** Curves fitting of the corrosion data of cold-rolled steel in the presence of inhibitors to Langmuir isotherm

solution on the cold-rolled steel obeys the Langmuir adsorption isotherm where,

$$\theta = \frac{KC}{KC + 1} \quad (10)$$

with

$$K = \left( \frac{1}{55.5} \right) \exp\left( -\frac{\Delta G_{\text{ads}}}{RT} \right) \quad (11)$$

where  $K$  is the equilibrium constant for the adsorption process,  $C$  is the concentration of the inhibitor and  $\theta$  is the surface coverage, 1 when inhibition efficiency is 100%.

The values of equilibrium adsorption constant obtained from these isotherms are about  $3.65 \times 10^5$  and  $1.87 \times 10^4 \text{ M}^{-1}$  for NPTU and DPTU, respectively, suggesting a chemically adsorbed film [35]. This is in good agreement with values of inhibition efficiency obtained from the electrochemical measurements. Therefore, inhibition efficiency increases with increasing equilibrium constant. Moreover, the largest negative values of  $\Delta G_{\text{ads}}$ , i.e. 42.38 kJ/mol for NPTU and 34.83 kJ/mol for DPTU, indicate that these inhibitors are strongly adsorbed onto the cold-rolled steel surface.

We can note that a plausible mechanism of corrosion inhibition of cold-rolled steel in 0.5 M  $\text{H}_2\text{SO}_4$  for compounds under study may be deduced on the basis of adsorption. In acidic solutions, these inhibitors can exist as cationic species which may be adsorbed on the cathodic sites of the cold-rolled steel and reduce the evolution of hydrogen. Moreover, the adsorption of these compounds on anodic sites through lone pairs of electrons of nitrogen, and sulfuric atoms and through  $\pi$ -electrons of C=S, phenyl and naphthyl groups will then reduce the anodic dissolution of cold-rolled steel, especially in the case of NPTU.

Further insight into the adsorption mechanism is offered by careful look at the curves in Figs. 2 and 3. From Fig. 3 it can be seen that the increasing of the concentration of DPTU leads to the apparition of the irregularity of anodic polarization current, for example, for the concentration of  $2.5 \times 10^{-4} \text{ M}$  of DPTU the anodic current is greater than that corresponding to concentration of  $10^{-4} \text{ M}$ . Meanwhile, Fig. 3 reveals that the cathodic polarization curves follow a same regular tendency when the concentration of DPTU increases. The irregularity observed in the anodic region is probably due to modification in the adsorbed DPTU on the surface. The most probable modification of the DPTU inhibitor, which is responsible for the increase in anodic current at  $2.5 \times 10^{-4} \text{ M}$  is the protonation process. The protonation of DPTU results in the attachment of a proton to the highly negative S-atom

[36]. So, it is expected that both unprotonated and protonated species of DPTU could exist in acid solution. Due to electrostatic attraction, the cationic species may adsorb on the cathodic sites of cold-rolled steel and reduce the evolution of hydrogen and thereby protecting the cathodic sites of steel. The adsorption of DPTU at anodic sites can be attributed to the presence of unprotonated molecular species. Increasing of the inhibitor concentration ( $>10^{-4} \text{ M}$ ) probably increases the protonated species on the surface [37] and so, decreases the cathodic currents and increases the anodic currents. This could explain the strange anodic behavior of DPTU at different concentrations. Note that the irregularity observed in the case of DPTU at higher concentrations does not occur in the presence of NPTU (Fig. 2). Additional  $\pi$ -electrons in the naphthyl group, which increase the delocalization, may be the reason for this behavior. Owing to increase of delocalization, the  $\pi$ -electrons of naphthyl group are easily translated to Fe atoms. When this effect is prevalent compared to that of protonation, the final result is a decrease of anodic current.

In summary, the results show that NPTU is more efficient than DPTU, this may be due to the highest molecular weight and the presence of additional naphthyl group.

#### Effect of temperature

The effect of temperature variation on inhibitor efficiency is important in practical applications. It is essential therefore to study this in order to obtain an indication of the inhibitive efficiency at height temperature as well as at room temperature.

The behavior of cold-rolled steel in 0.5 M  $\text{H}_2\text{SO}_4$  aqueous solution in the absence and in the presence of NPTU and DPTU at  $10^{-4} \text{ M}$  during polarization was studied in the 293–323 K temperature range. The corresponding data are given in Table 4.

We remark that the rise in temperature leads to an increase in corrosion rate with and without inhibitors. It can be seen from Table 4 that the inhibitor efficiencies increase with temperature.

The activation energy can be determined from Arrhenius plots for cold-rolled steel presented in Fig. 8 by the following relation:

$$\ln I_{\text{corr}} = -\frac{E_A}{RT} + \ln A \quad (12)$$

where  $E_A$  represent the apparent activation energy,  $R$  is the universal gas constant,  $T$  is the absolute temperature and  $A$  is the pre-exponential factor.

The regression between  $\ln I_{\text{corr}}$  and  $1/T$  was completed by using computer, and it is found that the regression coefficients are very close to 1, which means that the linear relationship between  $\ln I_{\text{corr}}$  and  $1/T$  is good.

The apparent activation energies for the corrosion in the absence and presence of NPTU and DPTU can be calculated from the slopes of the regression and are respectively:

$$E_A = 77.87 \text{ kJ/mol}, \quad E'_A = 33.36 \text{ kJ/mol}$$

and

$$E''_A = 35.31 \text{ kJ/mol}$$

We remark the decrease in activation energy in the presence of the inhibitors studied. The Influence of temperature on corrosion inhibition was studied by several authors [6, 38–40] who reported that the activation energy is lower for the inhibited than for the uninhibited reaction. This was attributed to increased surface coverage of the metal surface with the inhibitor molecule with increasing temperature. On the other hand, the decrease in  $E_a$  in inhibited solution support the assumption for chemisorption of the inhibitor on the metal surface [41]. Moreover, Szauer, Brandt and Foroulis [42, 43] declare that the lower activation energy value of the process in the presence of the inhibitor compared to that of in its absence is attributed to its chemisorption, while the opposite is the case with physical adsorption.

Table 4 shows also that the inhibition efficiency ( $P\%$ ) increases with the increase of the temperature of corrosion medium. This result can be explained by the characteristics of the cathodic process of hydrogen evolution in acidic solutions. The hydrogen evolution overvoltage decreases with increasing temperature that

**Table 4** Effect of temperature on the inhibition efficiency and electrochemical parameters of the cold-rolled steel in 0.5 M  $\text{H}_2\text{SO}_4$  with and without NPTU and DPTU at  $10^{-4}$  M

	$T$ (K)	$E_{\text{corr}}$ (mV/SCE)	$I_{\text{corr}}$ ( $\mu\text{A cm}^{-2}$ )	$b_c$ (mV dec $^{-1}$ )	$P$ (%)
Blank	293	-488	851	163	–
	303	-490	2140	179	–
	313	-500	9770	210	–
	323	-483	12300	270	–
NPTU	293	-485	45	148	94.7
	303	-503	95.5	178	95.5
	313	-490	141	185	98.6
	323	-485	158.4	192	98.7
DPTU	293	-520	263	136	69.1
	303	-520	480	143	77.6
	313	-511	730	162	92.5
	323	-520	966	166	92.1

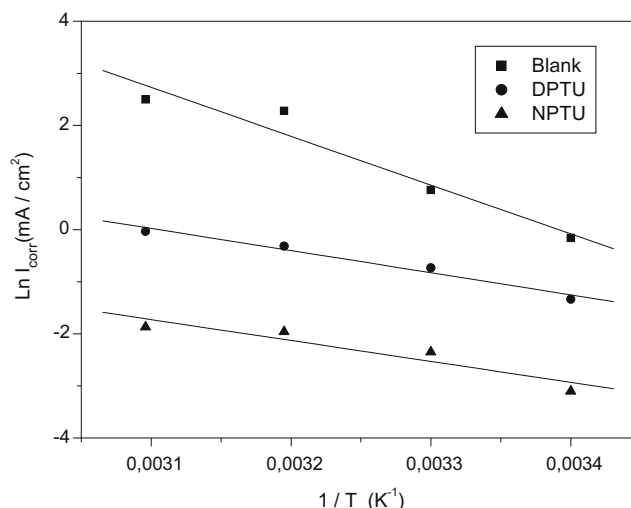


**Fig. 8**  $\ln I$  versus  $1/T$  for cold-rolled steel dissolution in 0.5 M  $\text{H}_2\text{SO}_4$  in the presence and in the absence of  $10^{-4}$  M NPTU and DPTU

leads to increase in the cathodic reaction rate. On the other hand, temperature increase accelerates the chemisorption of the inhibitor of the metal surface. When the latter effect is predominant, the final result is an increase of the inhibiting effect, which is observed in this work.

### Theoretical calculations

It was shown from the electrochemical and weight loss measurements that the substitution of phenyl group by naphthyl group leads to increase the inhibition efficiency. The inhibition efficiency depends on many factors [44] including the number of adsorption centers, mode of interaction with metal surface, molecular size and structure.

In order to give further insight into the experimental results, ionization potentials are computed and the Fukui indices are used for predicting the preferential sites of electrophilic attack on DPTU and NPTU. It is known that the Fukui indices were widely used as descriptors of site selectivity for the soft–soft reactions [45, 46]. According to Li–Evans [47], the favorite reactive site is that which possesses a high value of Fukui indice. Hence, relationships between electronic structure and efficiency of DPTU and NPTU can be deduced from Fukui indices calculations. In this way, we have calculated the electrophilic Fukui indices  $f_k^-$ , defined by Eq. 2, for heteroatoms in the two systems. The results are given in Table 5. It turns out from the tabulated values that the sulfur atom, in DPTU and NPTU, possesses the largest value of Fukui indices



**Table 5** Calculated Fukui indices

Heteroatom	Fukui indices	
	NPTU	DPTU
N1	0.036	0.039
N2	0.023	0.040
S	0.108	0.107

(0.107 and 0.108 for DPTU and NPTU, respectively). Thus, the sulfur atom is more reactive for electrophilic attack than nitrogen atoms in the two systems. Indeed, the nitrogen atoms, in both DPTU and NPTU systems have very small values of electrophilic Fukui indices (less than 0.041). These results seem to indicate that the S atom, which has a great nucleophilic character, is involved in the chemical reactivity of these molecules with the metal surface while the N atoms of the two compounds seem not to participate in the reactivity [48]. However, the substitution of phenyl group by naphthyl group in the DPTU molecule does not affect the Fukui indices of the S atom and consequently its reactivity. Thus, the increase of the inhibition efficiency can be attributed mainly to the additional  $\pi$ -electrons in the naphthyl group that then reduce the ionization potential (the values of the potential ionization of DPTU and NPTU are 7.202 and 7.050 eV, respectively). According to Koopmans' theorem [49] the ionization potential ( $I$ ) of a molecule is simply the orbital energy of the highest occupied molecular orbital with the inverse sign ( $I = -E_{\text{HOMO}}$ ). We note that the outer  $\pi$ -electrons of the naphthyl group are higher in energy compared to those of the phenyl group. Obviously, the increase of the energy of outer  $\pi$ -electrons yields to the decrease of the ionization potential. Thus, the lower the ionization potential (the higher the  $E_{\text{HOMO}}$ ) of organic molecules, the easier is it to offer electrons to unoccupied d orbitals of metals and the higher is the inhibition efficiency. In summary, we can conclude that the inhibition effect is due mainly to the ionization potential.

This result is consistent with the conclusion of Stoyanova and Peyerimhoff [50] that there is a clear relation between the increase in corrosion inhibition and the decrease of the ionization potential.

## Conclusions

It can be concluded as follows:

- The thiourea derivatives were found to perform in 0.5 M, but the better performance was seen in the case of NPTU.

- Polarization studies showed that the compounds under investigation were mixed type inhibitors.
- The inhibition efficiency of the thiourea derivatives increased with the concentration and reached a maximum at  $2 \times 10^{-4}$  M.
- The weight loss, electrochemical impedance spectroscopy, polarization curves and linear polarization were in good agreement.
- Adsorption of NPTU and DPTU on the steel surface from 0.5 M  $\text{H}_2\text{SO}_4$  followed the Langmuir isotherm.
- $P\%$  of NPTU and DPTU increased with increasing temperature and their addition led to a decrease of the activation corrosion energy.
- The substitution of phenyl group by naphthyl group in the DPTU molecule was very beneficial towards inhibition of corrosion of cold-rolled steel in 0.5 M  $\text{H}_2\text{SO}_4$ .
- The inhibition efficiency increased with increasing of the adsorption equilibrium constants value.
- Theoretical calculation results reveal that the substitution of phenyl group by naphthyl group in the DPTU molecule does not affect the Fukui indices of the S atom and that the better inhibition efficiency obtained by NPTU can be explained in terms of ionization potential.

## References

1. Bentiss F, Traisnel M, Gengembre L, Lagrenée M (1999) *Appl Surf Sci* 152:237
2. Bentiss F, Lagrenée M, Traisnel M, Gornez JC (1999) *Corros Sci* 41:789
3. El kanouni A, Kertit S, Srhiri A, Ben Bachir A (1996) *Bull Electrochem* 12:517
4. Mernari B, Elattari H, Traisnel M, Bentiss F, Lagrenée M (2002) *Corros Sci* 40:573
5. Ramesh S, Rajeswari S (2004) *Electrochim Acta* 49:811
6. Touhami T, Aounti A, Abed Y, Hammouti B, Kertit S, Ramdani A, Elkacemi K (2000) *Corros Sci* 42:929
7. Algaber AS, El-Nemna EM, Saleh MM (2004) *Mater Chem Phys* 86:26
8. Branzoi V, Branzoi F, Baibarac M (2000) *Mater Chem Phys* 65:288
9. Quraishi MA, Sardar R, Jamel D (2001) *Mater Chem Phys* 71:309
10. Oguzie EE, Unaegbu C, Okolue CBN, Onuchukwu AI (2004) *Mater Chem Phys* 84:363
11. Oguzie EE, Onuoha GN, Onuchukwu AI (2005) *Mater Chem Phys* 89:305
12. Annand RR, Hurd RM, Hackerman N (1965) *J Electrochem Soc* 112:138
13. Abo El Khair MB, Mostafa B, Khalifa OR, Abdel-hamid IA, Azzam AM (1987) *Corros Prev Control* 34:152
14. Abed Y, Hammouti B, Touhami F, Aouniti A, Kertit S, Mansri A (2001) *Bull Electrochem* 17:105

15. Larabi L, Harek Y, Traisnel M, Mansri A (2004) *J Appl Electrochem* 34:833
16. Harek Y, Larabi L (2004) *Kem Ind* 53:55
17. Ameer MA, Khamis E, Al-Senani G (2002) *J Appl Electrochem* 32:149
18. Quarraishi MA, Jamal D, Singh RN (2002) *Corrosion* 58:201
19. Singh A, Chaudhary RS (1996) *Br Corros J* 31:300
20. Ita BF, Offiong OE (1999) *Mater Chem Phys* 59:179
21. Parr RG, Yang W (1989) In: *Density-functional theory of atoms and molecules*. Oxford University Press, Oxford
22. Dewar MJS, Zoebisch EG, Healy EF (1985) *J Am Chem Soc* 107:3902
23. Stewart JJP (1990) *J Comput Aided Mol Des* 4:1
24. Gaussian 94 (Revision D.1), Frisch MJ, Trucks GW, Schlegel HB, Gill PMW, Johnson BG, Robb MA, Cheeseman JR, Keith TA, Petersson GA, Montgomery JA, Raghavachari K, Al-Laham MA, Zakrzewski VG, Ortiz JV, Foresman JB, Peng CY, Ayala PY, Wong MW, Andres JL, Replogle ES, Gomperts Rn, Martin RL, Fox DJ, Binkley JS, Defrees DJ, Baker J, Stewart JP, Head-Gordon M, Gonzalez C, Pople JA (1995) Gaussian Inc., Pittsburgh, PA
25. Mulliken RS (1955) *J Chem Phys* 23:1833
26. Cheng XL, Ma HY, Chen SH, Yu R, Chen X, Yao ZM (1999) *Corros Sci* 41:321
27. Bockris JO'M, Yang B (1991) *J Electrochem Soc* 138:2237
28. Hukovic-Metikos M, Babic R, Grutac Z (2002) *J Appl Electrochem* 32:35
29. Mansfeld F (1981) *Corrosion* 37:301
30. Mccafferty E (1997) *Corros Sci* 39:243
31. Wu X, Ma H, Chen S, Xu Z, Sui A (1999) *J Electrochem Soc* 146:1847
32. Ma H, Chen S, Yin B, Zhao S, Liu X (2003) *Corros Sci* 45:867
33. Hackerman N, Mccafferty E (1974) In: *Proceedings of the fifth international congress on metallic corrosion*. Houston, TX, p 542
34. Zvauya R, Dawson JL (1994) *J Appl Electrochem* 24:943
35. Villamil RFV, Corio P, Rubin JC, Agostinho SML (2002) *J Electroanal Chem* 535:75
36. Pillai KC, Narayan R (1983) *Corros Sci* 23:151
37. Awad MK (2004) *J Electroanal Chem* 567:219
38. Putilova IN, Balezin SA, Barannik VP (1960) In: *Metallic corrosion inhibitors*. Pergamon Press, New York
39. Stoyanova AE, Sokolova EI, Raicheva SN (1997) *Corros Sci* 39:1595
40. Lagrenée M, Mernari B, Bouanis M, Traisnel M, Bentiss F (2002) *Corros Sci* 44:573
41. Sankarapapavinasam S, Pushpanaden F, Ahamed M (1991) *Corros Sci* 32:193
42. Szauer T, Brandt A (1981) *Electrochim Acta* 26:1209
43. Foroulis ZA (1990) in *Proceedings of the 7th European corrosion inhibitors*. Ferrara, pp 149
44. Mohamed AK, Raha TH, Moussa NNH (1990) *Bull Soc Chim Fr* 127:375
45. Ayers PW, Levy M (2000) *Theor Chem Acc* 103:353
46. Geerlings P, De Proft F (2002) *Int J Mol Sci* 3:276
47. Li Y, Evans JNS (1995) *J Am Chem Soc* 117:7756
48. Cruz J, Martínez R, Genesca J, García-Ochoa E (2004) *J Electroanal Chem* 566:111
49. Koopmans T (1933) *Physica* 1:104
50. Stoyanova AE, Peyerimhoff SD (2002) *Electrochim Acta* 47:1365